

Flux-Assisted Double Perovskite Ba₂CuTaO₆ Electrodes with Ultralow Charge-Transfer Resistance for High-Rate Supercapacitors

Hassan Idris Abdu ^{1,*}, Taslim Aboudou ¹, Yi Liu ¹, Huili Wang ¹, and Sefiu Abolaji Rasaki ^{2,*},

¹ College of Health Management, Shangluo University, Shangluo, 726000, Shaanxi, China

² Department of Chemical and Petroleum Engineering, University of Calgary, AB, T2N 1N4, Canada

Corresponding Authors

*Email: hassan.idris@slxy.edu.cn; sefiu.rasaki@ucalgary.ca

Supporting information

S1. Microstructure and phase analysis of reference perovskites

CuTaO₄ forms anisotropic nanorods (Figure 2a,b), typical of Ta₂O₅-templated 1D growth in KCl flux, where Cl⁻ coordination stabilizes rod-like nuclei. HRTEM (Figure 2c) exposes lattice fringes $d(111) = 0.31$ nm (monoclinic I2/m), and SAED (Figure 2d) confirms single-crystallinity with no twinning—flux suppresses stacking faults common in Ta-oxides (defect density $<10^{16}$ cm⁻³). EDS maps (Figure 2e,f) show stoichiometric Cu:Ta:O = 1:1:4 uniformity, with Cu²⁺ enrichment at rod tips suggesting surface segregation that enhances local redox activity ¹. BaTaO₄ aggregates into sub-micron spheres (Figure 2g,h), hierarchical porosity from CO₂ effervescence during BaCO₃ decomposition, amplified by flux Ostwald ripening. HRTEM/SAED (Figure 2i,j) reveal orthorhombic Pnma phase with $d(200) = 0.28$ nm. Elemental maps (Figure 2k,l) confirm Ba:Ta:O ~1:1:4, though slight Ba surface excess (~5 at%) indicates mild segregation reducing bulk conductivity. Compared to flux-free CuTaO₄ (irregular 1–5 μm chunks, $R_{ct} > 10$ Ω), KCl processing yields nanostructuring that boosts surface area ~15-fold, correlating with 2× higher C_{sp} in rods vs. spheres. These morphologies establish baseline perovskites where Ba₂CuTaO₆'s ordered B-site doping will show

synergy ².

S2. Surface chemistry of CuTaO₄ and BaTaO₄

CuTaO₄ XPS shows Cu 2p_{3/2} (933.2 eV) with prominent shake-up satellite (941.5 eV, Figure 4A), diagnostic of paramagnetic Cu²⁺ in distorted octahedra, consistent with monoclinic distortion enhancing Jahn-Teller effects for redox accessibility. Ta 4f (Figure 4B) doublet (26.0/28.0 eV) confirms Ta⁵⁺ stability, while O 1s (Figure 4C) shifts hydroxyl fraction to 38% (531.3 eV) higher than Ba₂CuTaO₆ due to Cu-induced surface hydroxylation, promoting Ta⁵⁺/Ta⁴⁺ minor contributions ².

Surface oxidation states and hydroxyl groups enable reversible pseudocapacitive charge storage. BaTaO₄ Ba 3d (778.8/794.4 eV, Figure 4D) and Ta 4f (Figure 4E) match literature Ba²⁺/Ta⁵⁺, but O 1s (Figure 4F) reveals lower lattice O²⁻ (48%, 529.5 eV) and elevated defect oxygen (32%, 531.5 eV), reflecting orthorhombic vacancy tolerance that traps ions, explaining inferior kinetics later. Across compositions, Cu presence correlates with higher M–OH (~35% avg), boosting pseudocapacitance via OH⁻ insertion (E_{reaction} ~0.4 V). Flux washing preserves ~20% more active surface vs. solvent-free, aligning with 1.5× C_{sp} gains in Cu-containing perovskites.

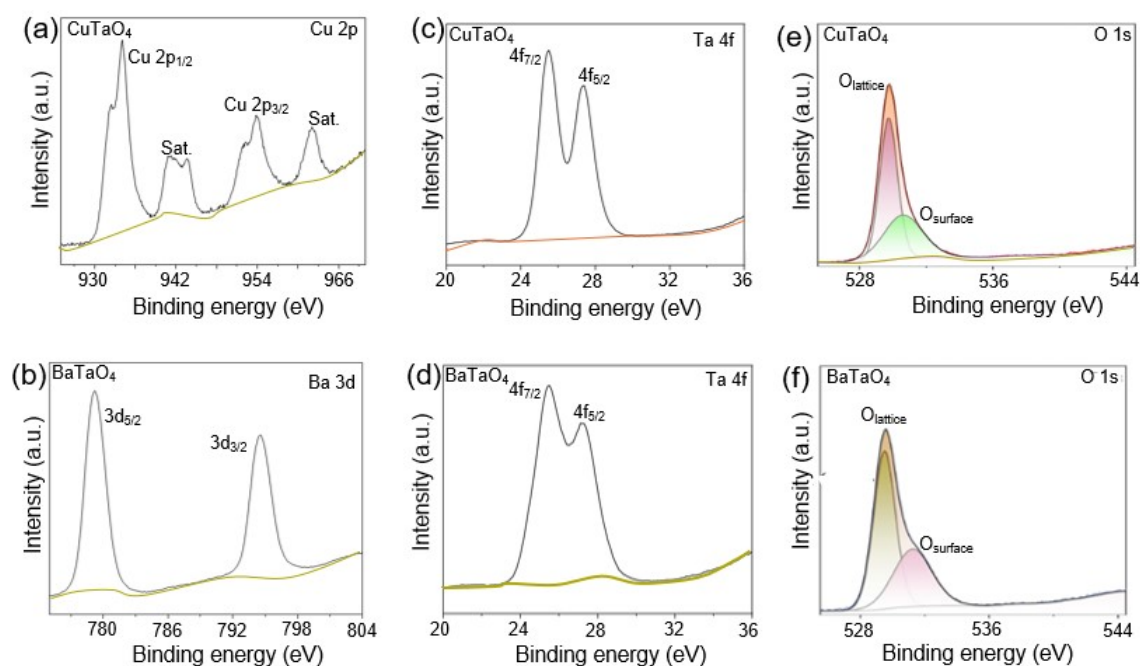


Figure S1: High-resolution XPS spectra of CuTaO₄ and BaTaO₄. (a-c) CuTaO₄: (a)

Cu 2p showing Cu²⁺ 2p_{3/2} and 2p_{1/2} with shake-up satellites; (b) Ta 4f revealing Ta⁵⁺ 4f_{7/2} and 4f_{5/2}; (c) O 1s deconvoluted into lattice oxygen (O²⁻), and surface hydroxyl. BaTaO₄: (d) Ba 3d; (e) Ta 4f; (F) O 1s deconvoluted into oxygen species.

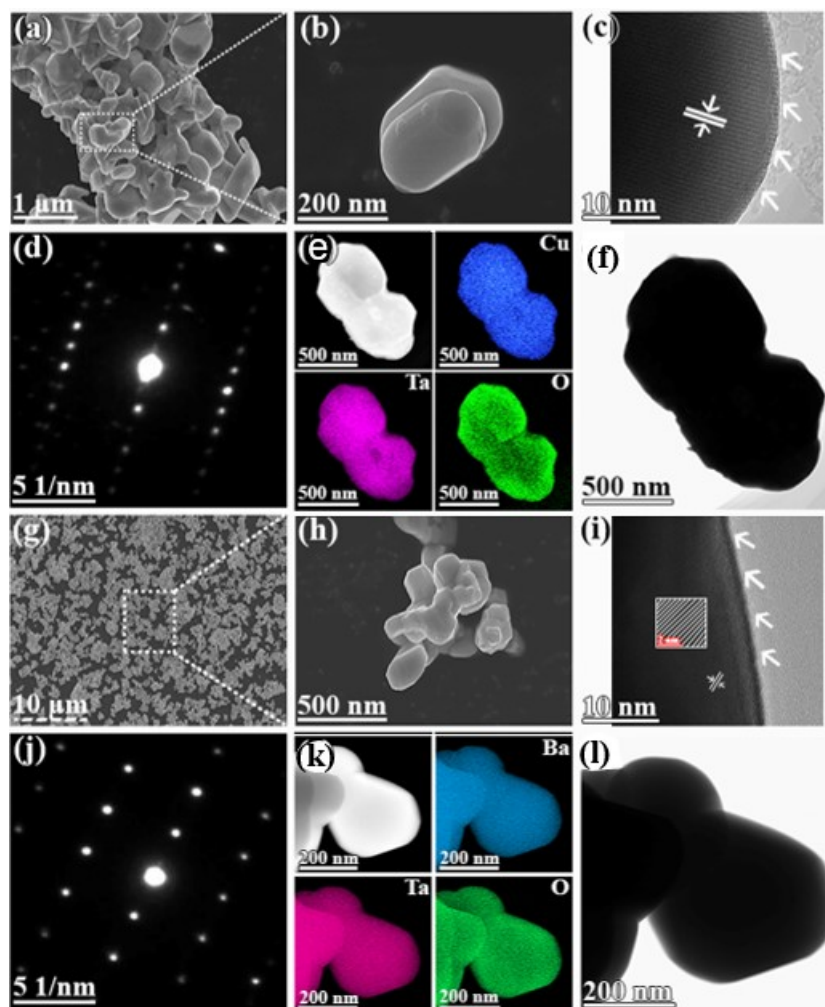


Figure S2: Supporting structural/surface data for reference perovskites. Microstructure, crystallinity and elemental distribution of flux-assisted solid-state synthesized CuTaO₄ and BaTaO₄. (a, b) SEM images of CuTaO₄ at different magnifications. (c) HRTEM image of CuTaO₄ (inset: enlarged lattice region). (d) SAED pattern of CuTaO₄. (e, f) TEM image and corresponding EDS elemental maps (Cu, Ta, O). (g, h) SEM images of BaTaO₄ at different magnifications. (i) HRTEM image of BaTaO₄. (j) SAED pattern of BaTaO₄. (k, l) TEM image and corresponding EDS elemental maps (Ba, Ta, O). Flux-assisted synthesis ensures phase purity and crystalline order.

Table S1: Crystallinity of the as-prepared materials

Material	Crystallinity (%)
CuTaO ₄	95.5
BaTaO ₄	96.2
Ba ₂ CuTaO ₆	98.7

Reference

1. Y. Su, Y. Tsujimoto, K. Fujii, M. Tatsuta, K. Oka, M. Yashima, H. Ogino and K. Yamaura, *Inorganic Chemistry*, 2018, **57**, 5615-5623.
2. S. A, J. Kunjumon, A. K. Jose, A. P. A, M. Tomy, W. Akram, R. P. Jebin, X. T. S, T. Maity and D. Sajan, *Ceramics International*, 2024, **50**, 15756-15766.